

# New empirical constraints on the cosmological evolution of gas and stars in galaxies

Hamsa Padmanabhan<sup>1\*</sup> and Abraham Loeb<sup>2†</sup>

<sup>1</sup> Canadian Institute for Theoretical Astrophysics, 60 St. George Street, Toronto, ON M5S 3H8, Canada

<sup>2</sup> Astronomy department, Harvard University, 60 Garden Street, Cambridge, MA 02138, USA

Accepted —. Received —; in original form —

## ABSTRACT

We combine the latest observationally motivated constraints on stellar properties in dark matter haloes, along with data-driven predictions for the atomic (HI) and molecular (H<sub>2</sub>) gas evolution in galaxies, to derive empirical relationships between the build-up of galactic components and their evolution over cosmic time. We find that at high redshift ( $z \gtrsim 4$ ), galaxies acquire their cold gas (both atomic and molecular) mostly by accretion, with the fraction of cold gas reaching about 20% of the cosmic baryon fraction. We find a strong dependence of the star formation rate on the H<sub>2</sub> mass, suggesting a near-universal depletion timescale of 0.1–1 Gyr in Milky Way sized haloes (of masses  $10^{12} M_{\odot}$  at  $z = 0$ ). We also find evidence for a near-universality of the Kennicutt-Schmidt relation across redshifts, with very little dependence on stellar mass, if a constant conversion factor ( $\alpha_{\text{CO}}$ ) of CO luminosity to molecular gas mass is assumed. Combining the atomic and molecular gas observations with the stellar build-up illustrates that galactic mass assembly in Milky-Way sized haloes proceeds from smooth accretion at high redshifts, towards becoming merger-dominated at late times ( $z \lesssim 0.6$ ). Our results can be used to constrain numerical simulations of the dominant growth and accretion processes of galaxies over cosmic history.

**Key words:** galaxies: star formation - galaxies: evolution - galaxies: high-redshift

## 1 INTRODUCTION

The so-called ‘baryon cycle’ in galaxies offers novel insights into the inter-relationship between gas and stellar evolution across cosmic time. While we do not yet have a complete picture of the details of galaxy formation (for a review, see, e.g., Naab & Ostriker (2017)), some of the outstanding questions include: (i) the relative contributions of mergers and smooth accretion to the gas assembly in galaxies (e.g., Kereš et al. 2005; Dekel et al. 2009; Nelson et al. 2013), as a function of halo mass and cosmic time, (ii) whether the physical processes governing star formation at high redshifts differ from those in the local universe, and (iii) the precise roles of atomic (HI) and molecular (H<sub>2</sub>) gas (e.g., Daddi et al. 2010a; Tacconi et al. 2013; Saintonge et al. 2017) in driving the cosmological star formation rate.

Various semi-analytical and simulation methods have been used to predict the cosmological evolution of gas and stars in galaxies. While Semi-Analytical Methods (SAMs; e.g. Guo et al. 2010; Benson 2012; Somerville et al. 2008; Popping et al. 2014; Somerville & Davé 2015) use sophisticated prescriptions having free parameters to model the physical parameters associated with the gas, stellar, black hole and radiation associated with galax-

ies, detailed hydrodynamical codes (e.g., Naab & Ostriker 2017; Tacchella et al. 2019) explicitly simulate these processes in a cosmological setting. Analytical techniques, such as toy models (e.g., Dekel et al. 2013; Lilly et al. 2013) offer a complementary sketch for the stellar and gas build-up.

An alternative approach to constrain galaxy evolution is the empirical (data-driven) framework, in which observationally measured quantities are used to set direct constraints on the properties of gas and stars in haloes. For the  $\Lambda$ CDM cosmological scenario, several empirical studies have placed constraints on the stellar properties in galaxies across cosmic time (e.g., Behroozi et al. 2013c; Moster et al. 2013; Girelli et al. 2020; Tacchella et al. 2018; Behroozi et al. 2019) such as the stellar mass - halo mass (SHM) relation, using the technique of *abundance matching*. Such methods have been extended to atomic and molecular gas in Popping et al. (2015) by using physical prescriptions connecting gas profiles and stellar masses of galaxies. For atomic gas (HI) in galaxies, Padmanabhan et al. (2017) used the combination of presently available data from galaxy surveys, HI intensity mapping experiments and Damped Lyman Alpha (DLA) observations to constrain an empirical HI mass - halo mass relation (HIHM). The inferred HIHM was found to be characterized by three free parameters and does not evolve strongly with redshift. In Padmanabhan & Kulkarni (2017), an equivalent, local HIHM was derived by matching the abundances of HI galaxies (at  $z \sim 0$ ) observed in the HIPASS sur-

\* Email: hamsa@cita.utoronto.ca

† Email: aloeb@cfa.harvard.edu

vey (Zwaan et al. 2005a) to the mass function of dark matter haloes (Sheth & Tormen 2002).<sup>1</sup>

The primary observational tracer of molecular gas ( $H_2$ ) is carbon monoxide (CO) which is strongly connected to the star formation rate. In Padmanabhan (2018), constraints on the CO luminosity function at low redshifts (Keres et al. 2003) were combined with intensity mapping observations at  $z \sim 3$  from the CO Power Spectrum Survey (COPSS; Keating et al. 2016) to predict the evolution of the CO luminosity - halo mass ( $L_{CO} - M$ ) relation via abundance matching. The observations were found to be consistent with a well-defined  $L_{CO} - M$  having four free parameters, motivated by the empirical SHM of Moster et al. (2013). In contrast to the HIHM, the inferred  $L_{CO} - M$  is observed to show a significant evolution across  $z \sim 0 - 4$ .

The extended Press-Schechter (EPS) formalism provides a convenient framework to compute the assembly history of a given dark matter halo via mergers of smaller haloes (Sheth & Tormen 2002). Merger trees computed from numerical simulations (e.g., Klypin et al. 2011) allow the tracking of the most massive (main) progenitor halo for a given halo across cosmic time. In this paper, we combine the empirically determined prescriptions connecting the stellar (Behroozi et al. 2013c, 2019), atomic (Padmanabhan et al. 2017) and molecular (Padmanabhan 2018) gas in galaxies to haloes, with the merger tree framework that describes halo assembly, to provide an understanding of the growth histories of the various galactic components and their dependences on each other. This analysis extends previous work to construct ‘baryon progenitor trees’ which are directly motivated by observations. In so doing, it sheds light into the relative contributions of mergers and smooth accretion to gas mass assembly, and the dependence of the star formation history on the atomic and molecular gas depletion timescales.<sup>2</sup> Being completely empirical, this study is free from the uncertainties involved in physical models of stellar and gas evolution in galaxies. As such, it provides an important benchmark for calibrating the detailed physics in current and forthcoming simulations of galaxy formation, and enables the understanding of the dominant processes involved therein.

The outline of this paper is as follows. In Sec. 2, we present the formalism which associates gas to dark matter haloes, which we connect to the empirical framework for the evolution of the stellar component in Sec. 3. Finally, Sec. 4 summarizes our main results.

## 2 HALO MODEL FRAMEWORKS FOR ATOMIC AND MOLECULAR GAS

In this section, we briefly review the existing empirical frameworks developed for associating atomic and molecular gas to dark matter haloes. For atomic gas (HI), we use the halo model for cosmological neutral hydrogen (Padmanabhan et al. 2017), which combines constraints from HI galaxy surveys at  $z \sim 0$  (Zwaan et al. 2005a,b;

Martin et al. 2010, 2012; Braun 2012), intensity mapping experiments (around  $z \sim 1$ ; e.g. Switzer et al. 2013) and the statistics of Damped Lyman Alpha (DLA) systems (column density distributions, incidences and three dimensional clustering: Rao et al. 2006; Prochaska & Wolfe 2009; Noterdaeme et al. 2012; Font-Ribera et al. 2012; Zafar et al. 2013) across  $z \sim 0 - 5$ . The results of a joint fit to all these datasets favour a well-defined mean HI mass - halo mass relation:

$$M_{HI}(M, z) = \alpha_{HI} f_{H,c} M \left( \frac{M}{10^{11} h^{-1} M_{\odot}} \right)^{\beta} \times \exp \left[ - \left( \frac{v_{c0}}{v_c(M, z)} \right)^3 \right], \quad (1)$$

with the three parameters (i)  $\alpha_{HI} = 0.09 \pm 0.01$ , which denotes the average HI fraction relative to cosmic  $f_{H,c}$ , (ii)  $\beta = -0.58 \pm 0.06$ , the logarithmic slope of the relation which represents the deviation from linearity of the prescription, and (iii)  $v_{c0}$ , given by  $\log(v_{c,0}/\text{km s}^{-1}) = 1.58 \pm 0.04$  which denotes the minimum virial velocity below which haloes preferentially do not host HI.

To describe the molecular gas ( $H_2$ ) evolution, we use the results of Padmanabhan (2018), which infers a CO luminosity - halo mass relation having the physically motivated form:

$$L_{CO}(M, z) = 2N(z)M[(M/M_1(z))^{-b(z)} + (M/M_1(z))^{y(z)}]^{-1}, \quad (2)$$

with the parameters  $M_1(z)$ ,  $N(z)$ ,  $b(z)$  and  $y(z)$  themselves consisting of two terms - a constant term which describes the behaviour at  $z \sim 0$ , and an evolutionary component:

$$\begin{aligned} \log M_1(z) &= \log M_{10} + M_{11}z/(z+1); \\ N(z) &= N_{10} + N_{11}z/(z+1); \\ b(z) &= b_{10} + b_{11}z/(z+1); \\ y(z) &= y_{10} + y_{11}z/(z+1). \end{aligned} \quad (3)$$

The best fitting values for these parameters, found from fitting the observations of Keres et al. (2003) at  $z \sim 0$  are given by  $M_{10} = (4.17 \pm 2.03) \times 10^{12} M_{\odot}$ ,  $N_{10} = 0.0033 \pm 0.0016 \text{ K km/s pc}^2 M_{\odot}^{-1}$ ,  $b_{10} = 0.95 \pm 0.46$ ,  $y_{10} = 0.66 \pm 0.32$ . The evolutionary components, derived by subsequently matching the COPSS results (Keating et al. 2016) at  $z \sim 3$  are given by:

$$\begin{aligned} M_{11} &= -1.17 \pm 0.85; \\ N_{11} &= 0.04 \pm 0.03; \\ b_{11} &= 0.48 \pm 0.35; \\ y_{11} &= -0.33 \pm 0.24. \end{aligned} \quad (4)$$

The above framework can be converted into an equivalent  $H_2$  mass to halo mass evolution by assuming a CO luminosity -  $H_2$  mass conversion factor. The value of this factor - denoted by  $\alpha_{CO}$ , and defined through  $M_{H_2} = \alpha_{CO} L_{CO}$  (with  $M_{H_2}$  in units of  $M_{\odot}$  and  $L_{CO}$  in units of  $\text{K km/s pc}^{-2}$ ) - and its evolution are still observationally uncertain. Several studies (e.g., Bolatto et al. 2013) advocate the present value of  $\alpha_{CO}$  to be of order unity, and recent ALMA evidence (e.g. Cortese et al. 2017) indicating a higher fraction of molecular gas at high redshifts compared to atomic, may be consistent with a non-varying  $\alpha_{CO}$ . Throughout this work, we assume  $\alpha_{CO} = 0.8$  across all redshifts under consideration.<sup>3</sup>

<sup>3</sup> A decreasing trend of  $\alpha_{CO}$  with  $z$  may be advocated by the observational results of Carleton et al. (2017) - which find about a  $\sim 1$  dex decline in  $\alpha_{CO}$

<sup>1</sup> Combining the HIHM so derived with the SHM obtained by Moster et al. (2013) led to an inferred HI-stellar evolution which was consistent with various  $z = 0$  measurements: from the *Galex* Arecibo SDSS Survey (GASS; Catinella et al. 2010, 2013), COLD GASS (Saintonge et al. 2011b,a; Catinella et al. 2012), the HERA CO Line Extragalactic Survey (HERACLES; Leroy et al. 2009) and The HI Nearby Galaxy Survey (THINGS; Walter et al. 2008).

<sup>2</sup> Assembly bias and environmental effects are expected to be have a small to negligible effect on the halo models for baryonic gas, whose spatial extents are much smaller than the dark matter virial radius.

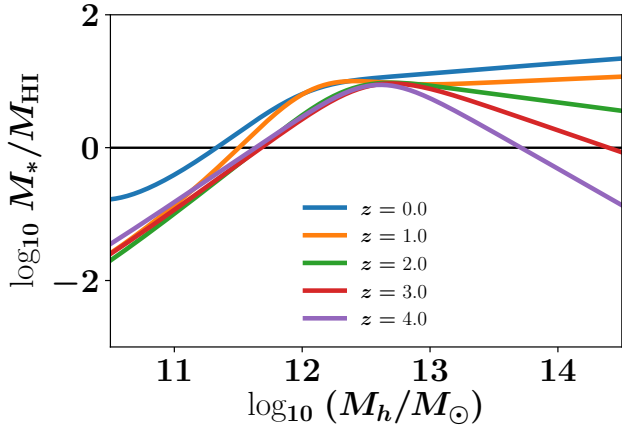


**Figure 1.** Empirically determined stellar-to-HI mass ratios ( $M_*/M_{\text{HI}}$ ) as a function of host halo mass  $M_h$ , and their evolution with redshift. A unit ratio is indicated by the black solid line.

### 3 BUILD-UP OF GAS AND STELLAR COMPONENTS

We can now combine the gas halo models outlined in Sec. 2 with the existing results linking stellar properties in galaxies with their host haloes. To do this, we use the results of Behroozi et al. (2019), who combine observational data collected from the Sloan Digital Sky Survey (SDSS), the PRISM Multi-object Survey (PRIMUS), UltraVISTA, the Cosmic Assembly Near-infrared Deep Extragalactic Legacy Survey (CANDELS), and the FourStar Galaxy Evolution Survey (ZFOURGE) over  $0 < z < 10.5$  to derive empirical constraints on the stellar mass to halo mass relation across cosmic time. We also use the publicly available catalogs of empirically determined star formation histories from Behroozi et al. (2013c) derived from a wide range of overlapping surveys over  $z = 0$  to 8.

It was found in Padmanabhan & Kulkarni (2017) that the local ( $z \sim 0$ ) HI-mass to stellar-mass ratio is about 25% in the rather broad range of halo masses from  $10^{11}$  to  $10^{13} M_\odot$  and decreases to about 10% at halo masses above this range. This behaviour can be extended to higher redshifts by combining the empirical HIHM of Padmanabhan et al. (2017) with the corresponding SHM derived by Behroozi et al. (2019). This is shown in Fig. 1 and indicates that the ratio of HI to stellar mass is fairly independent of redshift and only depends on halo mass.

Using the halo mass accretion histories from the *Bolshoi* simulations of Klypin et al. (2011) with haloes identified using the ROCKSTAR halo finder (Behroozi et al. 2013a) and the corresponding merger trees (Behroozi et al. 2013b), it is possible to construct the trajectory of the most massive progenitor halo at each redshift for a given halo at  $z = 0$ . Combining the merger trees and the empirical SHM relation (Behroozi et al. 2019) leads to the evolution of the stellar mass trajectories across cosmic time.<sup>4</sup> Corresponding trajectories for the gas mass build-up can be con-

between redshifts 0 and redshifts 3-4 (see also Bolatto et al. 2013). Since the detailed behaviour of  $\alpha_{\text{CO}}$  with redshift is essentially unconstrained, we prefer to stick with a non-varying value of  $\alpha_{\text{CO}}$  in the present work.

<sup>4</sup> The stellar mass build-up predicted by the most recent Illustris simulations (Fig. 6 of Tacchella et al. (2019)) are consistent with the findings of Behroozi et al. (2013c) at low redshifts if we consider the ‘star-forming’ component (although there is considerable scatter in the relation). The empirically predicted drop-off, however, may be somewhat steeper than that

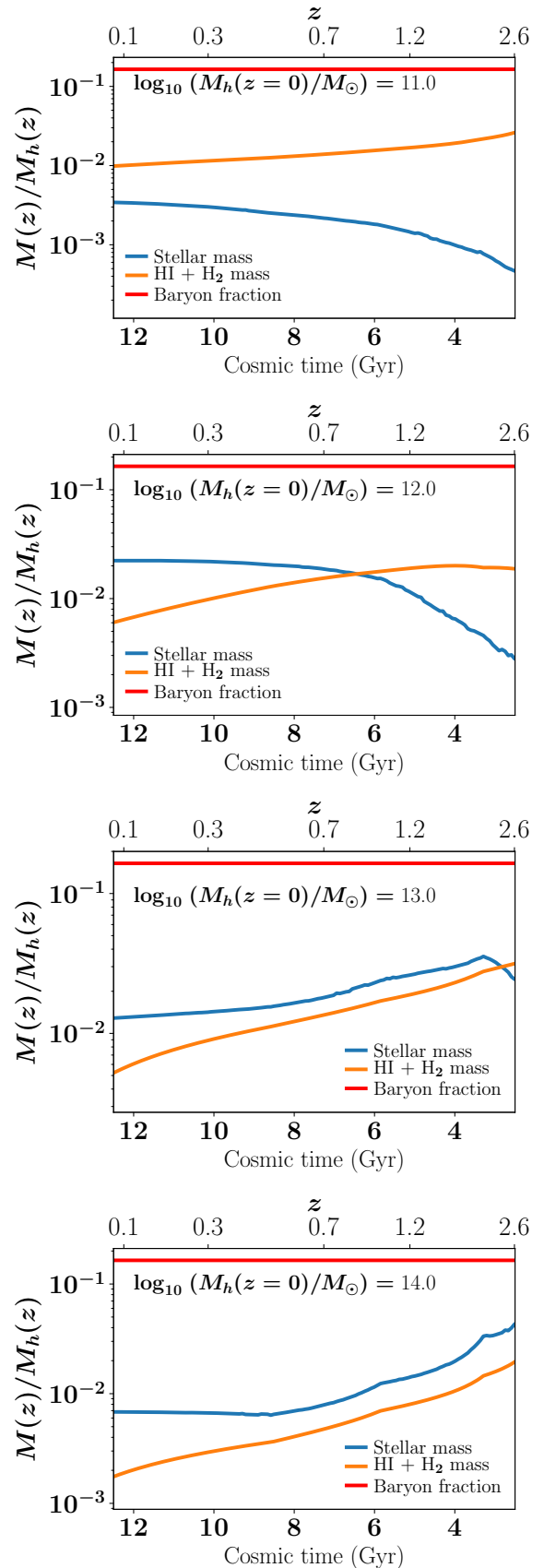


**Figure 2.** Build-up of gas (both HI and  $\text{H}_2$ ) mass, stellar and halo mass as a function of redshift (assuming a constant value of  $\alpha_{\text{CO}} = 0.8$  for converting CO luminosity to host halo mass). The plots show the ratio of the corresponding (stellar or gas) mass in galaxies to their host halo masses at different epochs. In all cases, the cosmological baryon fraction ( $f_b = \Omega_b/\Omega_m$ ) is shown by the solid red line.

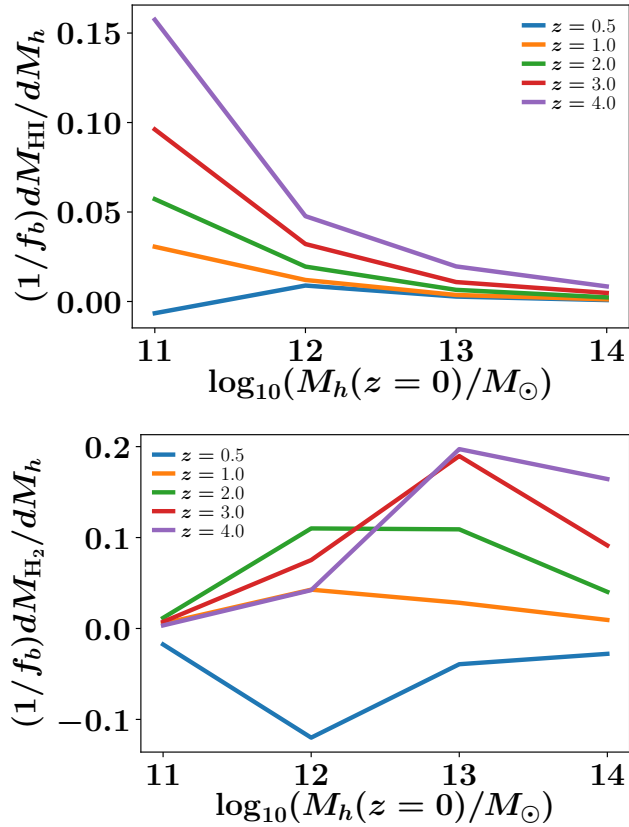


**Figure 3.** The fraction of cold gas mass accreted as a function of total halo mass at  $z = 0$ , for the main progenitor halo at various redshifts. The top panel indicates HI mass and the lower panel indicates the  $\text{H}_2$  mass using a constant  $\alpha_{\text{CO}} = 0.8$ .

structured by populating the merger trees with the gas-halo mass connections described in Sec. 2. These, along with the stellar build-up, are shown in Figs. 2 as a function of cosmic age, for four representative halo masses ( $10^{11} M_\odot$ ,  $10^{12} M_\odot$ ,  $10^{13} M_\odot$ , and  $10^{14} M_\odot$ ) at  $z = 0$ . The figures show that the star formation efficiency is highest in haloes of masses  $\sim 10^{12} M_\odot$ , with the stellar mass growing at the expense of the halo mass. These results are broadly consistent with those found in earlier semi-empirical studies: Behroozi et al. (2013c) and Popping et al. (2015), who use different prescriptions to connect atomic and molecular gas to stellar masses in galaxies. In all figures, the cosmological baryon fraction is plotted as the red solid line.

The two main modes of gas assembly in galaxies are by smooth accretion from the intergalactic medium (IGM) and mergers. Insight into smooth gas accretion may be gained by measuring what fraction of the baryon inflow turns into the atomic and molecular gas (HI and  $\text{H}_2$ ) of the central galaxy. This is plotted in the panels of Fig. 3 as a function of the host halo mass at  $z = 0$  (the curves show the trajectories for the most massive progenitor halo at different redshifts). The figures show that most of the cold gas is accreted at high redshifts ( $z \gtrsim 4$ ), reaching about 20% of the total baryon fraction.

The relative contribution of mergers and smooth accretion as

observed in the simulations at higher- $z$ , as seen from the right panel of Fig. 12 in Behroozi et al. (2013c).

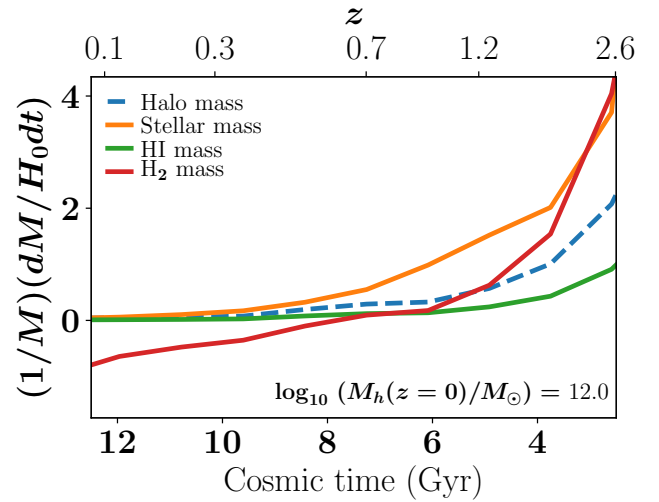


**Figure 4.** The evolution of gas (both HI and  $\text{H}_2$ ), stars and halo mass over cosmic time, using a constant ( $\alpha_{\text{CO}} = 0.8$ ) prescription to convert CO luminosity to molecular hydrogen mass.

a function of redshift can also be illustrated by plotting the derivatives of the gas and stellar fractions across cosmic time (normalized to the present-day Hubble constant). This is shown in Fig. 4 for a fiducial halo mass of  $10^{12} M_\odot$  at  $z = 0$ , and assuming a constant value of  $\alpha_{\text{CO}} = 0.8$ . The behaviour indicates that the stellar build-up follows the molecular gas at early times (where the orange and red curves are close to one another), but becomes merger-dominated at late times, following the halo mass evolution (where the orange curve is close to the blue dashed line). This is consistent with the simulations of L’Huillier et al. (2012) and the observational evidences collected by Sánchez Almeida et al. (2014), both of which indicate that smooth accretion, rather than mergers, is the dominant growth mode for gas mass assembly in the majority of high-redshift galaxies ( $z > 0.4$ ), whereas massive galaxies at lower redshifts are primarily merger-dominated. It can be shown that the average mass accretion rate into haloes of mass  $M_h$  at redshift  $z$  roughly follows the relation (Dekel et al. 2013, also discussed in Lilly et al. (2013); Davé et al. (2013)):

$$\frac{dM_h}{dt} \approx 30 M_{h,12}^{1.14} (1+z)^{2.5} M_\odot \text{ yr}^{-1}, \quad (5)$$

where  $M_{h,12} = M_h/10^{12} M_\odot$ . This can be simplified for massive haloes at  $z > 1$  to the form:

$$\frac{\dot{M}_b}{M_b} \simeq s(1+z)^{5/2}, \quad (6)$$

with  $s \sim 0.03 \text{ Gyr}^{-1}$ . Similar expressions are expected (Dekel et al. 2013) to hold for the baryonic accretion as well, which are consistent with the trends found in the present results.

### 3.1 Star formation and depletion timescales

Finally, we explore how the star formation history, whose connection to host halo mass is empirically constrained by the results of Behroozi et al. (2013c), depends on the build-up of the various components (atomic, molecular and stellar mass) above. The ratios of each of these components to their present-day values, are plotted in Fig. 5 as a function of redshift for a fiducial halo of mass  $10^{12} M_\odot$  at  $z = 0$ . The results indicate that the  $\text{H}_2$  mass closely

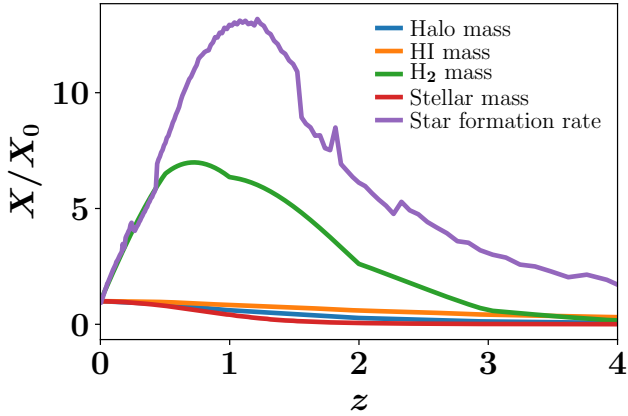


**Figure 5.** The build-up of star formation rate, gas (both HI and H<sub>2</sub>), stars and halo mass over cosmic time, as a function of its value at  $z = 0$ , using a constant ( $\alpha_{\text{CO}} = 0.8$ ) prescription to convert CO luminosity to molecular hydrogen mass. The curves correspond to a fiducial halo mass of  $10^{12} M_{\odot}$  at  $z = 0$ .

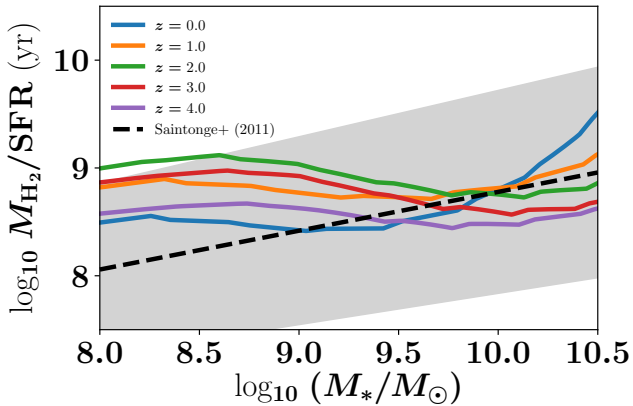


**Figure 6.** H<sub>2</sub> mass to SFR ratio, showing the depletion timescale for cold gas and its evolution with redshift and stellar mass. The fitting function derived by Saintonge et al. (2011b) at  $z \sim 0$  (which is based on observations of  $M_* > 10^{10} M_{\odot}$  galaxies) is plotted as the grey band. A constant  $\alpha_{\text{CO}} = 0.8$  is assumed when converting CO luminosity to H<sub>2</sub> mass.

traces the star formation rate as a function of cosmic time, with the peak of the SFR build-up occurring slightly earlier than that of the H<sub>2</sub> fraction relative to the present. Figure 6 shows the mean depletion timescale (H<sub>2</sub> mass to SFR ratio) across redshifts, as a function of the stellar mass. This is compared to the results of Saintonge et al. (2011b) for  $z \sim 0$  (which are based on measurements of  $M_* > 10^{10} M_{\odot}$  galaxies) and suggests an almost universal depletion timescale across redshifts, which is also consistent with the results found in earlier semi-empirical work (Popping et al. 2015). It also indicates empirical evidence for a lower value of  $\alpha_{\text{CO}}$  at higher redshifts than the present value (Bolatto et al. 2013), when compared with the observational findings of Daddi et al. (2010b); Genzel et al. (2010); Tacconi et al. (2013) which suggest that the depletion timescale may actually decrease with increasing redshift between  $z \sim 0 - 2$ .

## 4 DISCUSSION

We have developed several data-driven constraints on the build-up of atomic and molecular gas in galactic haloes, and their connections to observed stellar properties. This work brings together existing empirical constraints on the HI mass - halo mass relation and its evolution across redshifts (Padmanabhan & Kulkarni 2017; Padmanabhan et al. 2017), the luminosity and associated halo masses of CO-emitting galaxies across  $z \sim 0 - 4$  (Padmanabhan 2018) to calculate molecular gas mass evolution, and the observationally motivated stellar - halo mass (Behroozi et al. 2019) and star formation rate across the same epochs calibrated by Behroozi et al. (2013c). We find the following main results:

(i) The mean stellar/HI mass ratio is almost universal with redshift. The dependence of this ratio with stellar mass is consistent with the observations of Janowiecki et al. (2020) at  $z \sim 0$ , and indicates that the underlying physics may be independent of redshift and only depend on halo mass. This points to mergers as a possible mode of stellar and atomic gas build-up, which is consistent with the predictions of theoretical models at low redshifts for massive galaxies (e.g., Dekel et al. 2009).

(ii) At high redshifts, we find that most of the star formation is due to smooth accretion, rather than mergers, in Milky-Way sized haloes (of masses  $10^{12} M_{\odot}$  at  $z = 0$ ). This supports the ‘cold mode’ of gas accretion at high redshifts predicted by theoretical models (e.g., Dekel et al. 2009), and implies that most of the star formation is expected to take place in quiescent disk galaxies (e.g., Daddi et al. 2010b), rather than merger-driven starbursts at these epochs. It is also, in turn, consistent with the picture of extended galactic disks based on rest-frame UV/optical (e.g., Bell et al. 2005; Elbaz et al. 2007) and H $\alpha$  spectroscopy of galaxies (e.g., Genzel et al. 2008) and Damped-Lyman Alpha (DLA) system observations (e.g., Wolfe et al. 1986) at  $z \gtrsim 2$ .

(iii) The star formation is strongly connected to the molecular gas (H<sub>2</sub>) depletion timescale and negligibly to the atomic gas (HI). This reiterates the result, also found in Wang et al. (2020) advocating the role of HI only as an ‘intermediary’ in the process of star formation. It is also consistent with the arguments of Prochaska & Wolfe (2009) that point to a ‘self-correcting balance’ in atomic gas: the HI replenishment from the intergalactic medium being compensated by its conversion to H<sub>2</sub> which is consumed by star formation. This, in turn, is linked to the observed constancy of  $\Omega_{\text{HI}}$ , the HI density parameter across redshifts as measured from DLA studies and 21 cm experiments (for a compilation of recent observations, see Padmanabhan et al. (2015) and references therein).

(iv) The depletion timescale for the consumption of molecular gas,  $t_{\text{dep}} = (M_{\text{H}_2}/\text{SFR})$  is of the order of 0.1 - 1 Gyr, consistently with several observational results (e.g., Kennicutt 1983; Genzel et al. 2010) at  $z \sim 0 - 2$ . The  $t_{\text{dep}}$  does not depend strongly on stellar mass, which is consistent with recent observations (e.g., Janowiecki et al. 2020; Tacconi et al. 2018) at low redshifts. The trend is predicted to hold at higher redshifts as well, suggesting a universality in the Kennicutt-Schmidt relation (Kennicutt 1998). Taken together with the observations of Daddi et al. (2010a); Tacconi et al. (2013) and Genzel et al. (2010), this may provide evidence for a decreasing CO-to-H<sub>2</sub> conversion factor at high redshifts as compared to its current value.

The empirical constraints developed here serve as an important benchmark for calibrating the results of future simulations and semi-analytical models of galaxy formation that attempt to model the gas and stellar components in a self-consistent manner. Forth-

coming observations of atomic (e.g. with the SKA<sup>5</sup> and its precursors) and molecular gas (e.g. with the ALMA<sup>6</sup>/VLA<sup>7</sup>), as well as gravitational lensing surveys detecting cosmic shear, will be useful to further constrain the physical processes involved to provide a complete picture of galaxy evolution.

## ACKNOWLEDGEMENTS

HP thanks Dongwoo Chung and Mubdi Rahman for useful clarifications related to the empirical studies of stellar properties in dark matter haloes. The work of AL was supported in part by the Black Hole Initiative at Harvard University, which is funded by grants from JTF and GBMF.

## REFERENCES

- Behroozi P. S., Wechsler R. H., Wu H.-Y., 2013a, *ApJ*, **762**, 109
- Behroozi P. S., Wechsler R. H., Wu H.-Y., Busha M. T., Klypin A. A., Primack J. R., 2013b, *ApJ*, **763**, 18
- Behroozi P. S., Wechsler R. H., Conroy C., 2013c, *ApJ*, **770**, 57
- Behroozi P., Wechsler R. H., Hearin A. P., Conroy C., 2019, *MNRAS*, **488**, 3143
- Bell E. F., et al., 2005, *ApJ*, **625**, 23
- Benson A. J., 2012, *New Astron.*, **17**, 175
- Bolatto A. D., Wolfire M., Leroy A. K., 2013, *ARA&A*, **51**, 207
- Braun R., 2012, *ApJ*, **749**, 87
- Carleton T., et al., 2017, *MNRAS*, **467**, 4886
- Catinella B., et al., 2010, *MNRAS*, **403**, 683
- Catinella B., et al., 2012, *A&A*, **544**, A65
- Catinella B., et al., 2013, *MNRAS*, **436**, 34
- Cortese L., Catinella B., Janowiecki S., 2017, *ApJ*, **848**, L7
- Daddi E., et al., 2010a, *ApJ*, **713**, 686
- Daddi E., et al., 2010b, *ApJ*, **714**, L118
- Davé R., Katz N., Oppenheimer B. D., Kollmeier J. A., Weinberg D. H., 2013, *MNRAS*, **434**, 2645
- Dekel A., et al., 2009, *Nature*, **457**, 451
- Dekel A., Zolotov A., Tweed D., Cacciato M., Ceverino D., Primack J. R., 2013, *MNRAS*, **435**, 999
- Elbaz D., et al., 2007, *A&A*, **468**, 33
- Font-Ribera A., et al., 2012, *J. Cosmology Astropart. Phys.*, **11**, 59
- Genzel R., et al., 2008, *ApJ*, **687**, 59
- Genzel R., et al., 2010, *MNRAS*, **407**, 2091
- Girelli G., Pozzetti L., Bolzonella M., Giocoli C., Marulli F., Baldi M., 2020, arXiv e-prints, p. [arXiv:2001.02230](https://arxiv.org/abs/2001.02230)
- Guo Q., White S., Li C., Boylan-Kolchin M., 2010, *MNRAS*, **404**, 1111
- Janowiecki S., Catinella B., Cortese L., Saintonge A., Wang J., 2020, arXiv e-prints, p. [arXiv:2001.06614](https://arxiv.org/abs/2001.06614)
- Keating G. K., Marrone D. P., Bower G. C., Leitch E., Carlstrom J. E., DeBoer D. R., 2016, *ApJ*, **830**, 34
- Kennicutt R. C. J., 1983, *ApJ*, **272**, 54
- Kennicutt Jr. R. C., 1998, *ApJ*, **498**, 541
- Keres D., Yun M. S., Young J. S., 2003, *ApJ*, **582**, 659
- Keres D., Katz N., Weinberg D. H., Davé R., 2005, *MNRAS*, **363**, 2
- Klypin A. A., Trujillo-Gomez S., Primack J., 2011, *ApJ*, **740**, 102
- L’Huillier B., Combes F., Semelin B., 2012, *A&A*, **544**, A68
- Leroy A. K., et al., 2009, *AJ*, **137**, 4670
- Lilly S. J., Carollo C. M., Pipino A., Renzini A., Peng Y., 2013, *ApJ*, **772**, 119
- Martin A. M., Papastergis E., Giovanelli R., Haynes M. P., Springob C. M., Stierwalt S., 2010, *ApJ*, **723**, 1359
- Martin A. M., Giovanelli R., Haynes M. P., Guzzo L., 2012, *ApJ*, **750**, 38
- Moster B. P., Naab T., White S. D. M., 2013, *MNRAS*, **428**, 3121
- Naab T., Ostriker J. P., 2017, *Annual Review of Astronomy and Astrophysics*, **55**, 59
- Nelson D., Vogelsberger M., Genel S., Sijacki D., Kereš D., Springel V., Hernquist L., 2013, *MNRAS*, **429**, 3353
- Noterdaeme P., et al., 2012, *A&A*, **547**, L1
- Padmanabhan H., 2018, *MNRAS*, **475**, 1477
- Padmanabhan H., Kulkarni G., 2017, *MNRAS*, **470**, 340
- Padmanabhan H., Choudhury T. R., Refregier A., 2015, *MNRAS*, **447**, 3745
- Padmanabhan H., Refregier A., Amara A., 2017, *MNRAS*, **469**, 2323
- Popping G., Somerville R. S., Trager S. C., 2014, *Monthly Notices of the Royal Astronomical Society*, **442**, 2398a–2418
- Popping G., Behroozi P. S., Peebles M. S., 2015, *MNRAS*, **449**, 477
- Prochaska J. X., Wolfe A. M., 2009, *ApJ*, **696**, 1543
- Rao S. M., Turnshek D. A., Nestor D. B., 2006, *ApJ*, **636**, 610
- Saintonge A., et al., 2011a, *MNRAS*, **415**, 32
- Saintonge A., et al., 2011b, *MNRAS*, **415**, 61
- Saintonge A., et al., 2017, *ApJS*, **233**, 22
- Sánchez Almeida J., Elmegreen B. G., Muñoz-Tuñón C., Elmegreen D. M., 2014, *The Astronomy and Astrophysics Review*, **22**, 71
- Sheth R. K., Tormen G., 2002, *MNRAS*, **329**, 61
- Somerville R. S., Davé R., 2015, *ARA&A*, **53**, 51
- Somerville R. S., Hopkins P. F., Cox T. J., Robertson B. E., Hernquist L., 2008, *Monthly Notices of the Royal Astronomical Society*, **391**, 481
- Switzer E. R., et al., 2013, *MNRAS*, **434**, L46
- Tacchella S., Bose S., Conroy C., Eisenstein D. J., Johnson B. D., 2018, *ApJ*, **868**, 92
- Tacchella S., et al., 2019, *MNRAS*, **487**, 5416
- Tacconi L. J., et al., 2013, *ApJ*, **768**, 74
- Tacconi L. J., et al., 2018, *ApJ*, **853**, 179
- Walter F., Brinks E., de Blok W. J. G., Bigiel F., Kennicutt Jr. R. C., Thornley M. D., Leroy A., 2008, *AJ*, **136**, 2563
- Wang J., Catinella B., Saintonge A., Pan Z., Serra P., Shao L., 2020, arXiv e-prints, p. [arXiv:2001.01970](https://arxiv.org/abs/2001.01970)
- Wolfe A. M., Turnshek D. A., Smith H. E., Cohen R. D., 1986, *ApJS*, **61**, 249
- Zafar T., Péroux C., Popping A., Milliard B., Deharveng J.-M., Frank S., 2013, *A&A*, **556**, A141
- Zwaan M. A., Meyer M. J., Staveley-Smith L., Webster R. L., 2005a, *MNRAS*, **359**, L30
- Zwaan M. A., van der Hulst J. M., Briggs F. H., Verheijen M. A. W., Ryan-Weber E. V., 2005b, *MNRAS*, **364**, 1467

This paper has been typeset from a  $\text{\LaTeX}$  file prepared by the author.

<sup>5</sup> <https://www.skatelescope.org/>

<sup>6</sup> <https://almascience.nrao.edu/about-alma/alma-basics>

<sup>7</sup> <https://science.nrao.edu/facilities/vla/>